Molecular Crystals and Liquid Crystals
Publication details, including instructions for authors and subscription information:
http://www.tandfonline.com/loi/gmcl18

Anchoring Transitions

P. Pieranski [a] & B. Jerome [a]
[a] Laboratoire de Physique des Solides, Universite Paris-Sud, Bat. 570, 91404, Orsay, France

Version of record first published: 24 Sep 2006.

To cite this article: P. Pieranski & B. Jerome (1991): Anchoring Transitions, Molecular Crystals and Liquid Crystals, 199:1, 167-187

To link to this article: http://dx.doi.org/10.1080/00268949108030928

Mol. Cryst. Liq. Cryst., 1991, Vol. 199, pp. 167–187
Reprints available directly from the publisher
Photocopying permitted by license only

Printed in the United States of America

Anchoring Transitions

P. PIERANSKI and B. JEROME

Laboratoire de Physique des Solides Universite Paris-Sud, Bat. 510 91404 ORSAY France

(Received August 15, 1990)

Orienting action of solid surfaces on nematic liquid crystals is known as the anchoring.

An Anchoring Transition consists in a singular change in the anchoring direction due to a continuous variation of some thermodynamic and structural parameters characterizing a solid/nematic interface. The structure of the interface is in fact sensitive, for example, to variations of chemical potentials of substances composing the nematic phase and to structural modifications of the solid substrate (due, for example, to surface strains).

An anchoring transition can take place by a jump from one orientation to another. Such a transition has all static and dynamic characteristics of a phase transition of first-order (nucleation and growth of domains surrounded by walls etc.).

An anchoring transition can also have the critical character of a second-order phase transition (occurrence of fluctuations of orientation, divergent susceptibility to external fields).

Experimental examples of anchoring transitions occurring at the E9/crystal interfaces will be presented and discussed in more details.

A mean field theory can be used for construction of generic anchoring diagrams in Fourier space; the interfacial grand canonical potential can be decomposed into a limited Fourier series and the Fourier coefficients can be treated as independent variables in the search for the minima. The correspondence with experimental anchoring diagrams is established by introducing dependence of Fourier coefficients on the thermodynamic and structural parameters.

I. INTRODUCTION

Since the discovery by Mauguin and Grandjean[1,2] of orienting action of crystalline substrates on nematic liquid crystals, a great variety of experimental and theoretical contributions has been devoted to the phenomenon of the anchoring of liquid crystals at interfaces. The state of art in this very extended field has been reviewed several times[3–5] in the past. A new review is in preparation.[6]

I.1. Interest of Anchoring Transitions

The scope of the present paper is much more limited. We focus here only on two interrelated topics:

1. The faculty of anchorings to evolve when some parameters, controlling states of the interface, are changing.
2. Anchoring transitions, that is to say, singular changes in anchoring directions.

that seem to us to be of more general interest especially in context of interfacial

phase transitions. We think that anchoring transitions are examples of interfacial phase transitions relatively easy to detect and to quantify for the following reasons:

In problems of mutilayer adsorption,[7] besides the entropy s, there are the densities ρ of adsorbed species that are considered as the pertinent parameters determining the state of the interface and revealing, by singularities of their evolution, possible interfacial phase transitions.

Experimental detection of these surface excess densities s or ρ requires special methods sensitive enough to probe surface states in the presence of the adjacent bulk phases.

In the present case, however, the nematic phase itself acts as a detector of interfacial states; because of its broken symmetry, the whole nematic phase (which is not distorted when the torque $\vec{\Gamma}$ acting on the interface is zero) adopts an orientation identical to the anchoring direction $\vec{a}$ (Figure 1):

$$\vec{n}(z > \xi) = \vec{a} \tag{1}$$

Detection of the orientation of a macroscopic nematic layer of a macroscopic

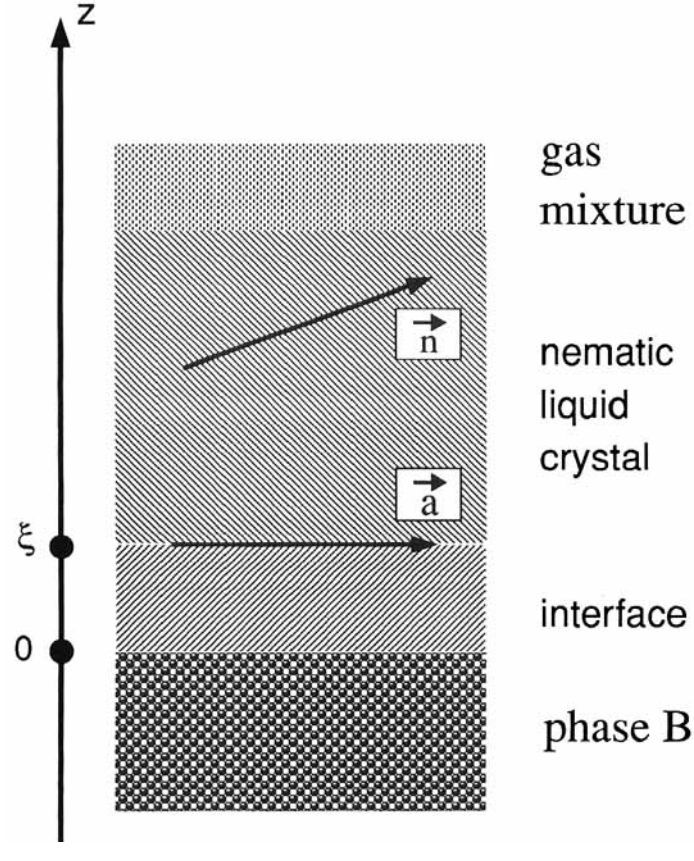

FIGURE 1 Schematic representation of an interface.

thickness d (much larger than ξ, defined in Figure 1) can be made by simple optical means such as using a polarizing microscope (see Figure 7 in section III.2.a.).

I.2. Introductory Remarks

Anchoring transitions were treated explicitly, so far, only in very few articles. Table I gives their summary. The structure of this table, that is to say, the choice of its entries reflects already our point of view which, here, is mainly phenomenological and uses general concepts of thermodynamics and symmetry.

From the second entry of the table results that changes in anchorings have been observed for a large variety of interfaces differing by composition and structure of the bulk phase in contact with the nematic LC.

We avoid discussion of all structural details by chosing as the principal criterium of classification the symmetry G_u (entry 4) of the interfacial thermodynamic potentials, defined in section II. We show there that once the symmetry group G_u is known, its subgroups G_a (entry 5) can be used for classification of possible types of anchoring.

From the third entry of the table results that several parameters can control anchorings. We show in section II that all these parameters can be treated as variables, describing conditions of the equilibrium between the interface and the adjacent bulk phases.

The most striking and crucial experimental facts mentioned in the entry 7 of the Table I are selectively presented in section III dealing with experimental aspects of anchoring transitions.

Finally, in section IV, we present some attempts of theoretical interpretation of anchoring transitions.

II. THERMODYNAMICS OF ANCHORING TRANSITIONS

Inspired by elegant theoretical approach of multilayer adsorption phenomena,[7] we consider the interface between the nematic phase and another phase as a thermodynamic system able to change its state as a function of some thermodynamic variables.

II.1. Parameters of the Interfacial States

Let Σ be a plane interface (of a fixed surface area A) between a nematic phase and another bulk phase. According to Gibbs,[8] such an interface should be seen as a thermodynamic system on its own, defined as a transition zone of thickness ξ, in which excess quantities such as:

- concentrations ρ_i of chemical species
- entropy s

are different from zero.

The state of the interface depends on thermodynamic intensive parameters such as:

TABLE I

Reference	13	14	18	16, 17	19, 21, 22	19, 21, 22	11
Nature of the interface	Nematic/crystal	Nematic/air	Nematic/ SiO film	Nematic/SiO film	Nematic/ gypsum	Nematic/muscovite	Nematic/ muscovite
Parameters of control	T	T	T	Evaporation angle	T, μ_{water}	T, μ_{water}, $\mu_{eth.glyc}$	Surface strain
Symmetry G_u of potentials		$C_{\infty v}$	C_s	C_s	C_2	C_s	C_s
Anchoring symmetries G_a	$C_{\infty v}$	$C_{\infty v}$, C_s	C_s, C_1	C_s, C_1	C_2	C_s, C_1	C_s, C_1
Anchoring transitions	Yes	2nd order	2nd order	2nd order	1st order	2nd and 1st order	1st order
Observations	Formation of an isotropic layer at the interface?			Anchoring selection during wetting[11]	Nucleation and growth of domains	Critical fluctuations	

- the chemical potentials μ_i
- the temperature T

set by the bulk phases that act, with respect to the interface, as reservoirs of heat or of particles.

Due to its specific structure, the nematic phase has the capacity to transmit

- a mechanical torque $\vec{\Gamma}$

to the interface. This occurs when the director field $\vec{n}(z > \xi)$ is not uniform. The quantity conjugated to the torque $\vec{\Gamma}$ is:

- the anchoring direction $\vec{n}(z = \xi) = \vec{a}$

defined as the orientation of the director at the interface. It has to be considered as another parameter, besides s and ρ_i, characterizing the state of the interface.

In the case when the nematic LC is in contact with a solid phase (such as a crystal), the last one can also be deformed by strains $\hat{e}$. Obviously, bulk strains must result in deformation of the crystal surface and affect the anchoring. Consequently,

- the surface strain tensor $\hat{e}$

should be considered as another parameter determining the state of the interface. However, when properly oriented, unlike the other parameters, the surface strain affects the symmetry of the interface. Therefore, in the following we will consider first in sections II.3.a, b and c situations of vanishing surface strains. Then, in section II.3.d, the surface deformation will be taken into account as a perturbation.

II.2. Definition of the Anchoring Transitions[9]

Variations of the intensive parameters μ_i and T characterizing the bulk phases should induce not only some modification of the conjugated extensive excess quantities ρ_i and s but also should change the anchoring direction $\vec{a}$.

One arrives at this conclusion by considering the internal energy of the interface:

$$u = u(\rho_i, s, \vec{a}) \tag{2}$$

which must be a function of the composition (represented by the densities ρ_i) and of the structure (related to the entropy s and to the anchoring direction $\vec{a}$) of the interface. Because the interface is in equilibrium with the bulk phases one has:

$$\frac{\partial u}{\partial \rho_i} = \mu_i \tag{3}$$

$$\frac{\partial u}{\partial s} = T \tag{4}$$

$$\frac{\partial u}{\partial \vec{a}} = \vec{\Gamma} \text{ (in following we set } \vec{\Gamma} = 0) \tag{5}$$

and the grand canonical potential of the interface defined by the equation:

$$\omega(\mu_i, T, \vec{a}) = u(\rho_i, s, a) - Ts - \rho_i\mu_i \tag{6}$$

must be in its minimum.

In the geometrical representation shown in Figure 2, the minimization of ω under conditions (3–5) corresponds to osculation of the surface $u = u(\rho_i, s, \vec{a})$ with a plane having slopes μ_i, T and $\vec{\Gamma}$ $(= \vec{0})$. It is clear that when the slope, say μ_i, of the osculating plane changes then not only the conjugated density ρ_i but also the anchoring direction (represented in Figure 2 by one angle) can vary.

It has been pointed out in Reference (9) that for some special shapes of the surface $u = u(\rho_i, s, \vec{a})$ the anchoring direction obtained by the above procedure can:

- Jump from one orientation to another; in such a case first-order anchoring transition takes place.
- Bifurcate; one gets a second-order anchoring transition.

Figure 3 shows examples of surfaces $u = u(\rho_i\, s, \varphi)$ (in topographic representation) leading to first-order (Figure 3a) and second-order (Figure 3b) anchoring transitions. Indeed, the procedure of osculation of the surface from Figure 3a gives as a result plots $\varphi = \varphi(\mu)$ and $\rho = \rho(\mu)$ shown in Figure 4a. Both functions show a discontinuity for $\tilde{\mu} = \mu - \mu_c = 0$. In the second case (Figure 4b corresponding to the Figure 3b) one gets, for μ^+ and μ^-, bifurcations of the anchoring angle and discontinuities of the slope $d\rho/d\mu$.

II.3. Symmetry Consideration

I.3.a. G_u; symmetry of thermodynamic potentials. The internal energy of the interface can be seen as a result of perturbation of intermolecular interactions in the nematic phase N by the phase B (or vice versa) (Figure 1). Therefore, the shape of the function $u = u(\rho_i, s, \vec{a})$ is not arbitrary but must be invariant with respect to:

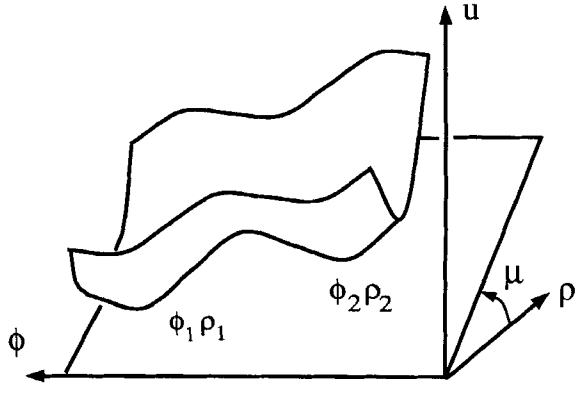

FIGURE 2 Geometrical interpretation of anchoring transitions.

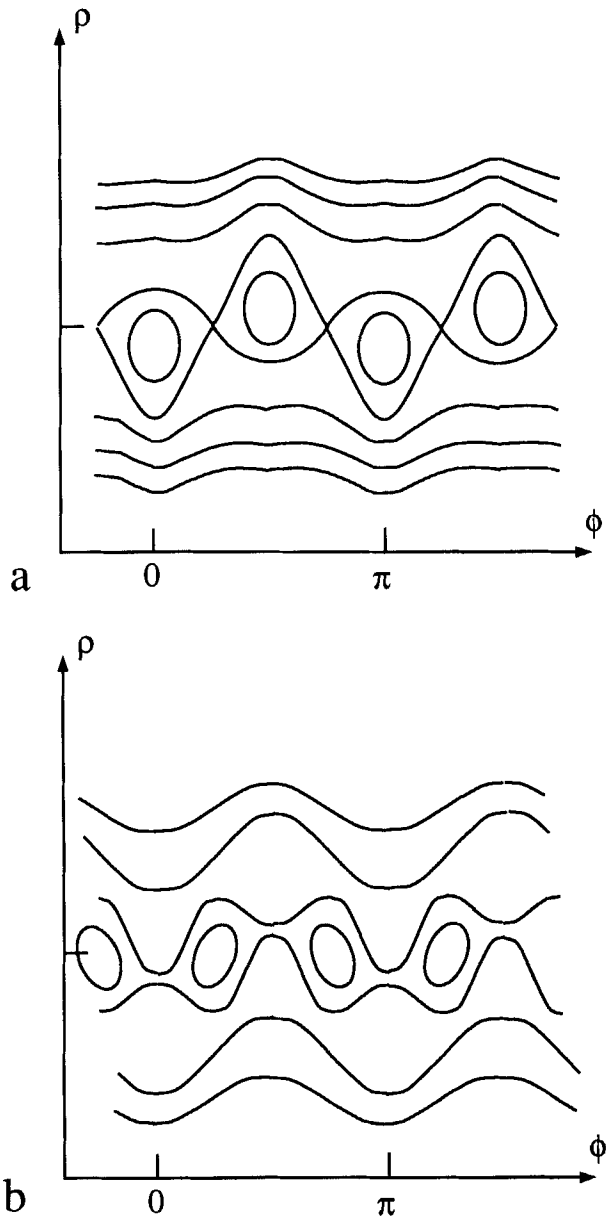

FIGURE 3 Plots of functions $u = u(\rho, \varphi)$ characteristic of: a) 1st-order anchoring transitions, b) 2nd-order anchoring transitions.

- Those of symmetry elements g of the phase B that transform its surface into itself.

In the case when the phase B is crystalline, this requirement limits the choice to those of symmetry axes C_2, C_3, C_4, C_6 and of mirror planes, that are perpendicular

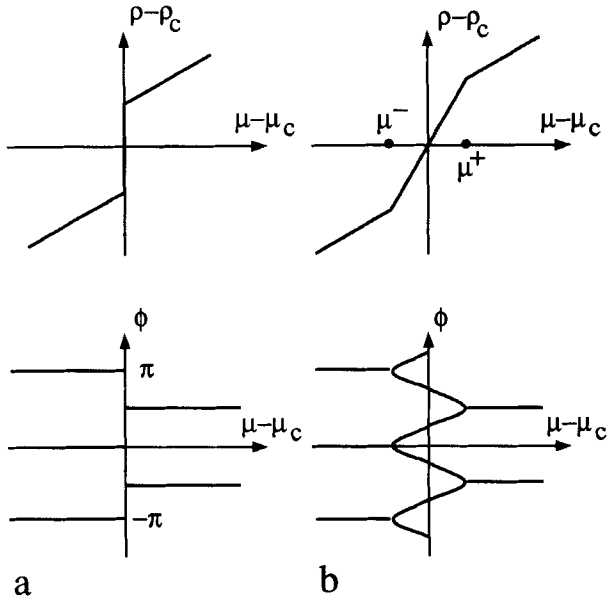

FIGURE 4 Plots of the anchoring angle φ (μ) and of the density ρ (μ) resulting from interfacial potentials shown in Figure 3.

to the interface. Such symmetry elements can be combined into ten point-symmetry groups of crystal surfaces.

The internal energy must be also invariant with respect to:

- The transformation $\vec{a} \Rightarrow -\vec{a}$.

characteristic of the nematic phase.

All other thermodynamic potentials such as the grand canonical potential ω (obtained from u by the Lagrange transform defined in Equation (3–5) and (6)), have the same symmetry such as u.

II.3.b. G_a; symmetry of the interface, type of the anchoring. Let $G_u = \{g\}$ be a symmetry group formed from above elements and characteristic of some interface.

The invariance of u with respect to G_u does not mean that the interface has necessarily the whole symmetry G_u. The actual symmetry of the interface depends on the orientation of the anchoring direction with respect to the symmetry elements of G_u.

Some special orientations of $\vec{a}$ can be invariant with respect to the whole group G_u.

For all other orientations, $\vec{a}$ is invariant only with respect to some subgroup G_a of G_u, and the interface, considered as a thermodynamic system on its own, has the symmetry G_a that is lower then G_u. In such a case the interface can be treated as a system with a broken symmetry. For a given symmetry G_u, its possible subgroups G_a (including G_u) define types of anchoring. Figure 5 shows different types of anchoring for $G_u = C_s$.

II.3.c. Symmetry changes at anchoring transitions. From above considerations

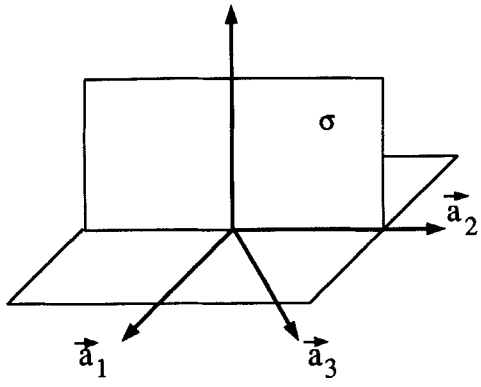

FIGURE 5 Types of anchorings possible for interfaces having the symmetry $G_u = C_s$: $\vec{a}_1$, $\vec{a}_2 - G_a = C_s$, $\vec{a}_3 - G_a = C_1$.

results that the symmetry rules valid for the usual phase transitions can be reformulated in the context of anchoring transitions as follows:

- Second-order anchoring transitions must involve a change of the type of anchoring G_a while for first-order anchoring transitions the type of anchoring is arbitrary.

This rule is illustrated by examples shown already in Figures 3 and 4. Indeed, let us consider φ as the azimuthal angle between the anchoring direction $\vec{a}$ and the mirror plane σ in the case when the group G_u is C_s (Figure 5). As required, the functions, shown in Figure 3 are invariant with respect to G_u. However, in the case of Figure 4b, for $\mu^- < \tilde{\mu} < \mu^+$, the anchoring direction is oblique with respect to the mirror plane so that the bifurcations occurring for μ^+ and μ^- correspond to breaking the mirror symmetry.

II.3.d. Multistable anchorings; anchoring selection. Let us consider a state of the interface characterized by an anchoring direction $\vec{a}_1$ such that the symmetry G_{a1} is broken with respect to G_u. All of the directions from the set defined by:

$$\{\vec{a}_1\}_u = \{g\vec{a}_1;\ g \varepsilon G_u\} \tag{7}$$

also satisfy the equilibrium conditions (3–5) and (6). In such a case, all anchoring directions belonging to the set $\{\vec{a}_1\}_u$ are equienergetic; their thermodynamic potentials ω defined by the Equation (6) are identical in the absence of torques $\vec{\Gamma}$. Therefore, in order to favor one of such equivalent states of the interface some action must be done.

Spreading patterns: As discussed in Reference (10), in the case of multistable anchorings on solid anisotropic substrates, the anchoring selection can be achieved during wetting of the substrate by the nematic liquid crystal; selection of the anchoring direction is a function of the wetting conditions, that is to say, of the direction of the contact line and of the (dynamical) contact angle. It has been shown that droplets, spread on the substrate, have a very characteristic pattern composed of domains, with all possibles anchoring directions from the set $\{\vec{a}_1\}_u$, and separated by walls. Examples of such patterns[10,25] are shown in Figures 6a, b, c.

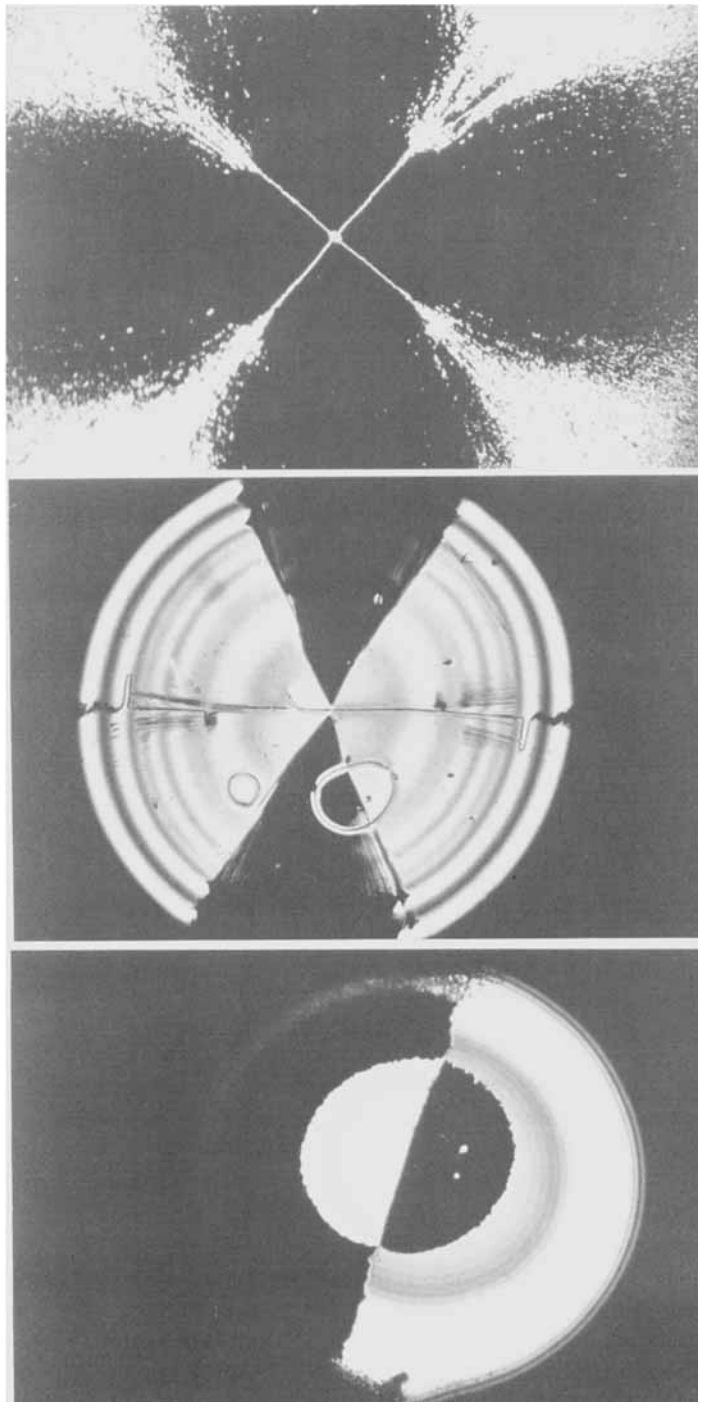

FIGURE 6 Spreading patterns on: (a)-(001) surface of silicon, (b)-phlogopite mica, (c)-SiO film. See Color Plate XII.

The mechanism of the anchoring selection during spreading of the droplets is dynamical and as such can not be discussed in terms of (equilibrium) quantities defined here.

Strain patterns[11]: Anchoring selection (and switching) can also be achieved by quasi-static processes such as, for example, application of a surface shear strain in the case of crystalline substrates. The shear strain deforms the surface of the crystal and breaks its symmetry,

In terms of the thermodynamic potential u (or ω) it means that it is modified in the presence of the strain by a perturbation δu:

$$u = u(\rho, s, \vec{a}) + \delta u(\rho, s, \vec{a}_\perp, \hat{e}) \tag{8}$$

where $\hat{e}$ is the bi-dimensional surface strain tensor and $\vec{a}_\perp$ is the bi-dimensional projection of $\vec{a}$ on the plane of the interface. When the perturbation δu is developed into powers of $\hat{e}$ then the lowest order term is

$$u = \delta u'(\rho, s)\vec{a}_\perp \cdot \hat{e} \cdot \vec{a}_\perp \tag{9}$$

Knowing that the most general expression for the shear strain field is:

$$\hat{e} = S_1 \begin{Bmatrix} 1 & 0 \\ 0 & -1 \end{Bmatrix} + S_2 \begin{Bmatrix} 0 & 1 \\ 1 & 0 \end{Bmatrix} \tag{10}$$

and that $\vec{a}_\perp$ can be written as

$$\vec{a}_\perp = a_\perp(\cos\varphi, \sin\varphi) \tag{11}$$

one gets from (9):

$$\delta u = \delta u'(\rho, s)\{S_1\cos(2\varphi) + S_2\sin(2\varphi)\} \tag{12}$$

or

$$\delta u = \delta u'(\rho, s)S\cos 2(\varphi - \psi)$$

where

$$S = (S_1^2 + S_2^2)^{1/2} \quad \text{and} \quad S_2/S_1 = \tan(2\psi). \tag{13}$$

By a proper orientation of eigen-axes of the strain, that is to say, by a proper choice of the angle ψ, one can favor any of the competing anchoring directions.

As pointed out in Reference (11), deformation field around a point-like inclusion must have a radial symmetry so that all possible strain directions are represented. The anchoring patterns realised on such strained substrates are similar to those in

spreaded droplets. Figure 11 shows an example of an anchoring pattern induced by strains in the vicinity of inclusions.

III. EXPERIMENTAL STUDIES OF ANCHORING TRANSITIONS

From phenomenological consideration of the previous section results that the state of the interface can be controlled, from outside, via the two adjacent bulk phases, by acting on "external" variables T, μ, and $\hat{e}$ characterizing these phases.

We have shown that in general, a change in one of these variables, all other being kept fixed, will shift the state of the interface into a new equilibrium at which of all "internal" parameters of the interface (u, s, ρ_i, $\vec{a}$) can change and not only the one that is conjugated to the modified external parameter. From the point of view of anchoring transition it means that changes in the anchoring direction can be triggered by any of the variables (T, μ_i, $\vec{\Gamma}$, $\hat{e}$).

We will show in following that this theoretical rule has been confirmed by experiments reporting occurrence of anchoring transitions, that is to say (singular) changes in the anchoring direction $\vec{a}$, under changes of all external parameters and not only of the torque $\vec{\Gamma}$.

III.1. Temperature-Dependent Anchoring Transitions

The temperature T is the parameter that was shown first[12,13] to trigger the anchoring transitions. Temperature-dependent anchoring transitions were found subsequently in other cases (see Table I). Let us discuss first studies where the temperature was the only one variable, among all possible external parameters, kept under control and where the anchoring transitions were found to occur at a temperature T_a close to bulk phase transitions.

III.1.a. Nematic/crystal interface wetted by the isotropic phase. In the case of the nematic/crystal interface,[13] the anchoring changes from a discrete one, for $T < T_a$, to an oblique (or planar) degenerate one for $T_{N/I} > T > T_a$, where $T_{N/I}$ is the temperature of the nematic-isotropic bulk phase transition.

Such a change in the type of the anchoring does not fit to the classification scheme developed in section II.3. The symmetry G_u of a crystal/nematic interface must be discrete what implies that for each type of anchoring, defined by subgroups G_a of G_u, the set of equivalent anchorings, defined in section II.3.d. should be discrete too. The degenerate anchoring violates this rule.

A possible explanation of this discrepancy is that an isotropic film of finite thickness builds up at the nematic/crystal interface in the temperature range $T_{N/I} > T > T_a$.[4] Then, instead of one nematic/crystal interface one should rather consider two interfaces; crystal/isotropic and isotropic/nematic. Now, the degenerate oblique (or planar) anchorings at the last interface are compatible with its symmetry $C_{\infty v}$.

Numerous articles were devoted to the problem of wetting of a nematic/solid interface by the isotropic phase (for $T < T_{N/I}$) or of an isotropic/solid interface by the nematic phase (for $T > T_{N/I}$).[15] Here, we will not discuss this problem in more details but we will focus only on interfaces having a molecular thickness.

III.1.b. Nematic/air interface. The nematic/air interfaces were studied extensively by Faetti *et al.*[14] They have shown that at the MBBA/air interface, the anchoring is tilted for $T < T_a < T_{N/I}$ and that the polar angle ϑ decreases with the temperature as $(T_a - T)^{1/2}$. Moreover, in this case, the anchoring transition is of the second order; the type of the anchoring changes from C_s to $C_{\infty v}$.

III.1.c. Nematic/rough-solid interface. A layer of SiO, evaporated on a glass substrate under oblique incidence has a columnar porous structure of symmetry C_s. Two types of anchorings, C_s and C_1, are a priori possible for this symmetry. It has been found that on such substrate the type of the anchoring can change as a function of the evaporation angle.[16,17] If the evaporation angle ε was treated as one of the parameters of the interface then the changes in the anchoring could be treated formally as anchoring transitions. It has been found by Braslau *et al.*[18] that in the case of octyloxy- and nonyloxybenzoic acids the anchoring transition between the C_s and C_1 types takes place also as a function of temperature. In this case the temperature of the anchoring transition is close to the nematic-smectic C bulk phase transition.

III.2. Chemical-Potential-Dependent Anchoring Transitions

In all above examples the vicinity of bulk phase transition suggests that these anchoring transitions correspond to (pretransitional) structural changes (entropy variations) of the interface rather than to changes in its composition (ρ).

In recent experiments, reported shortly below, besides the temperature T, also chemical potentials μ_i of several volatile compounds, such as water and ethylene glycol, were controlled. It has been found that anchoring transitions can occur at nematic/crystal interfaces also at constant temperature under variation of chemical potentials. Because, in such a case, changes in composition ρ_i of the interface must be involved, the anchoring transitions were qualified as adsorption-induced. (In fact, even in above cases of temperature-dependent anchoring transitions, variations of the composition cannot be excluded).

III.2.a. Set-up. Control of chemical potentials. The control of chemical potentials has been achieved by two different methods.

In the first one,[19] shown in Figure 7, a gas mixture, composed of nitrogene, water and/or other substances such as ethylene glycol, is slowly flowing above a sample. The sample is made of a thin, freshly cleaved crystal plate with a thin (a few micrometers) nematic layer spread on it. The composition of the gas mixture is set by means of flow-controllers regulating flows of dry nitrogen (Φ_{dry}) and of nitrogen saturated with vapors of water and/or other substances (Φ_i). In the approximation of ideal gas mixture, the partial pressures, given by:

$$p_i = p_s \frac{\Phi_i}{\Phi_{tot}}; \; \Phi_{tot} = \Phi_{dry} + \sum_i \Phi_i \tag{14}$$

determine the chemical potentials.

In the second method,[22] a similar sample is placed first in a vacuum chamber

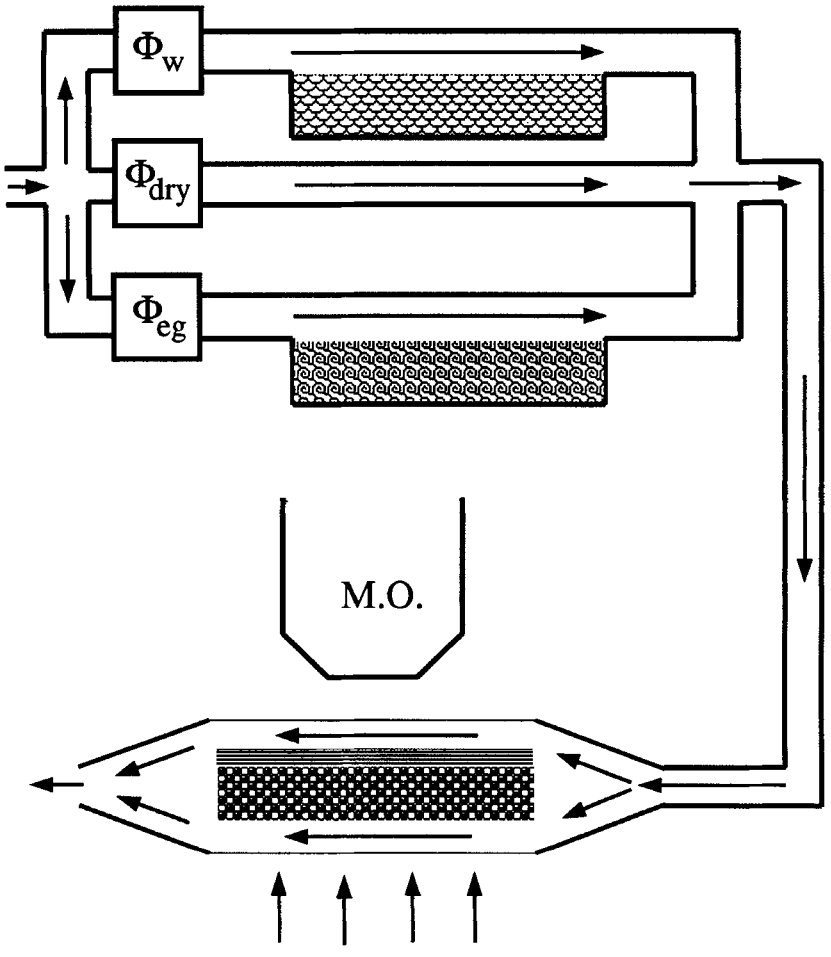

FIGURE 7 Experimental set-up for studies of adsorption-induced anchoring transitions.

and, then, a fixed amount of gas is introduced. Its pressure p_i is measured directly with a pressure transducer.

In these two methods, the equilibrium between the gas and the interface is reached by transport across the nematic layer. For thicknesses of the order of a few micrometers, the corresponding diffusion time is of the order of a few seconds.

III.2.b. Anchoring diagrams. Construction of anchoring diagrams consists in measuring the anchoring direction $\vec{a}$ as a function of the partial vapor pressures p_i, of chemical species composing the gas mixture above the nematic layer.

The function $\vec{a}\ (p_i)$ can have all kinds of singularities analog to those considered in the theory and practice of phase transitions. Let n be the dimension of the anchoring diagram, that is to say, the number of chemical species composing the gas mixture. Such an anchoring diagram may contain $(n-1)$-dimensional manifolds on which the function $\vec{a}\ (p_i)$ may have a discontinuity. When m of such first-order

manifolds meet, one gets a $(n - 2)$-dimensional manifold of m-tuple points. Such a $(n - 1)$-dimensional first-order manifold can terminate by a $(n - 2)$-dimensional manifold of critical points, etc.

Anchoring diagrams $\vec{a}$ (p_i) were explored already for several crystal substrates, liquid-crystal compounds and adsorbable impurities.[9,11,19–22]

As an example of a rich phenomenology, we show in Figure 8 the anchoring diagram of E9/muscovite interface in contact with a ternary mixture made of nitrogen and of vapors of water and ethylene glycol (containing traces of methanol).[20] As a reference for representation of (planar) anchoring directions, shown in inserts of the Figure 8, the plane σ of the approximate mirror symmetry, characterizing the mica surface, was chosen. The ternary diagram is divided in three domains I, II, and III by the transition lines AA′ and BB′. In the domain II the anchoring is parallel to the mirror σ, while in the domain I it is perpendicular to it. Upon crossing the BB′ line, from the domain I to the domain III, one observes a continuous bifurcation of the anchoring direction. In the domain III, two anchoring directions, oblique and symmetric with respect to σ can coexist.

If these two anchoring directions had the same stability, then the BB′ line would be a line of critical points, that is to say, a line of a second-order transition. Assuming that the symmetry C_s is perfect, the two anchoring directions would be

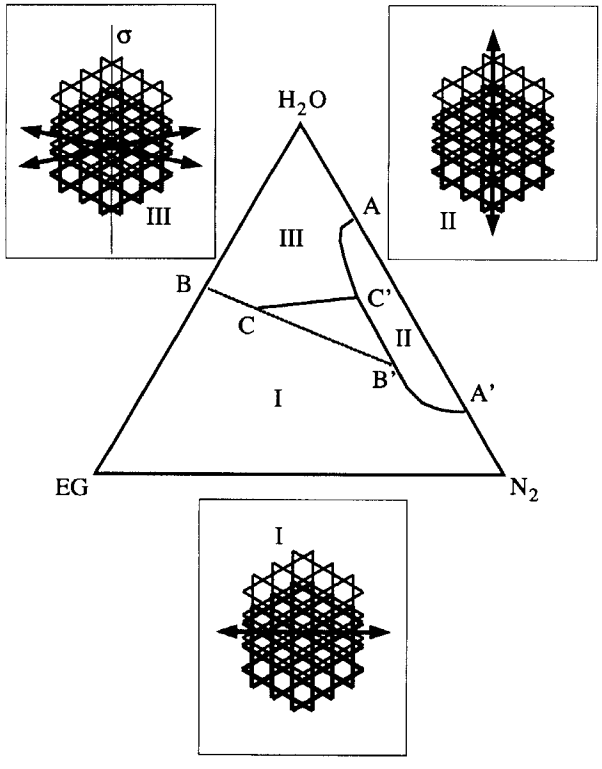

FIGURE 8 Anchoring diagram of a E9/muscovite interface in presence of vapors of water and ethylene glycol.

equivalent and the transition between domains I and III would correspond to the change of the type of anchoring from C_s to C_1. It is interesting to note that the transition from II to III involves the same symmetry breaking, but is of first order.

By a more accurate measurements one finds that, in fact, the domain III is divided by the line CC′. One side of this line, one of the two anchoring directions is more stable than the other one. On the other side of the line the situation is reversed. Therefore, the line CC′ is a line of a first-order anchoring transition and the point C is a critical point.

The presence of the line CC′ is due to imperfection of the mirror symmetry.

III.2.c. First-order anchoring transitions. Upon crossing the transition line AB′, between domains I and II, the anchoring direction changes by about 90 degrees. This first-order anchoring transition has all usual characteristics of first-order phase transitions. For example, it can proceed by different processes such as[21]:

1. Nucleation and growth of domains.
2. Splitting of walls.

The first of the two possibilities is illustrated in Figure 9. One observes the presence of elliptical walls separating growing areas with new anchoring direction (inside the elliptical domains) from the outside matrix with the "old" anchoring direction.

The second transformation mechanism of first-order anchoring transitions as well as other of their characteristics are discussed in more details in Reference (21).

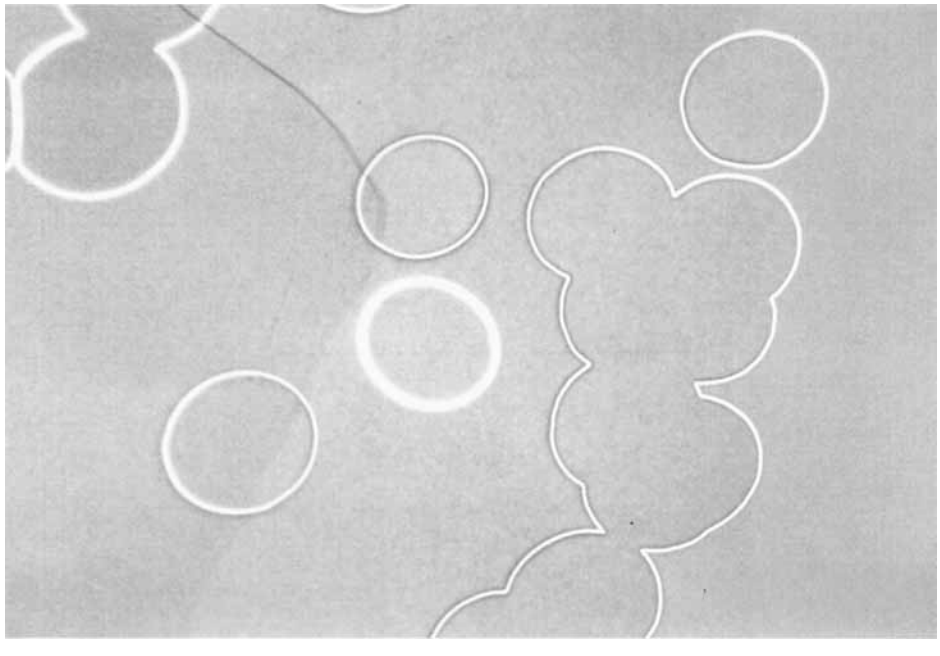

FIGURE 9 E9/muscovite interface. 1st-order anchoring transition: growth of domains. See Color Plate XIII.

III.2.d. Critical points, second-order transitions[20]. Besides the continuous variation of the anchoring direction, the most striking characteristics of critical points or of second-order anchoring transitions are critical fluctuations.

Observation of critical fluctuations in polarizing microscope should, in principle, be possible only very close to the transition point where the correlation length becomes of the order of light wave-length.

In spite of the fact that the partial pressures p_i are controlled with a relatively low accuracy (10^{-3}), critical fluctuations can be observed very easily. In Figure 10 we show a photograph of a E9/muscovite sample taken at the vicinity of the critical point C. Bright and dark domains, visible on the photograph, correspond to the two close anchoring directions, symmetrical with respect to the mirror plane and characteristic of the area III on the anchoring diagram in Figure 8. The wall, separating the domains with the two orientations, appears in the photograph as extremely irregular. When observed in the microscope, this wall fluctuates intensely.

III.3. Strain-Dependent Anchoring Transitions

Although fluctuating, the wall maintains an average position what means that choice of the two anchoring directions is not completely arbitrary on its two sides.

A plausible explanation of this fact, given recently by Kitzerow *et al.*,[11] is based on assumption that some residual strains can exist in the crystal substrate. As already discussed in section II.3.d, anchorings are sensitive to strains in crystal substrates especially in cases of multistable anchorings when more than one anchoring directions are equivalent. (By a proper orientation of the strain axes, one can favor any one of the competing anchoring directions). This is precisely the case

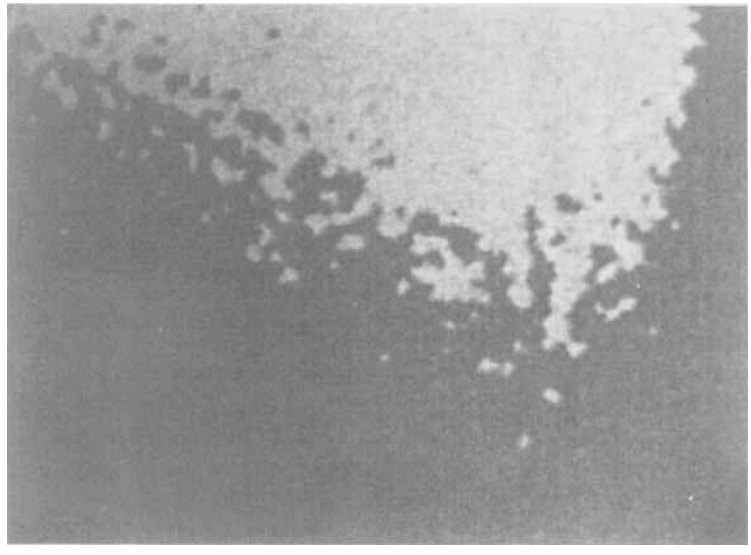

FIGURE 10 E9/muscovite interface. Critical fluctuations visible in polarizing microscope. See Color Plate XIV.

on the line CC′ where two anchoring directions coexist so that the pattern in Figure 10 may be due to some distribution of strains.

Confirmation of the action of strains, in the vicinity of the critical point C, is provided by the photograph in Figure 11. The strain field surrounding an inclusion has a radial symmetry. The butterfly-like anchoring pattern induced by such strain field is in agreement with theoretical predictions.

III.4. Torque-Dependent Anchoring Transitions

It has been shown[23,24] that in the case of multistable anchorings one can switch between the equivalent anchoring directions by applying an electric field of an appropriate direction to the nematic layer. Clearly, in these experiments, a torque is applied to the interface. The value and the direction of this torque is a function of the angle between the anchoring direction and the field. Such switching between two anchoring directions of the same type of anchoring is in fact not an anchoring transition in the rigorous meaning defined in section II.2.

IV. DISCUSSION AND CONCLUSIONS

In the introduction to adsorption-induced anchoring transitions (section.III.2.b.), anchoring transitions and other singularities were discussed in terms of m-dimensional manifolds embedded in n-dimensional space of thermodynamic variables $(T, \mu_i, \hat{e})$.

Due to the fact that, in principle, the same anchoring transition can be produced

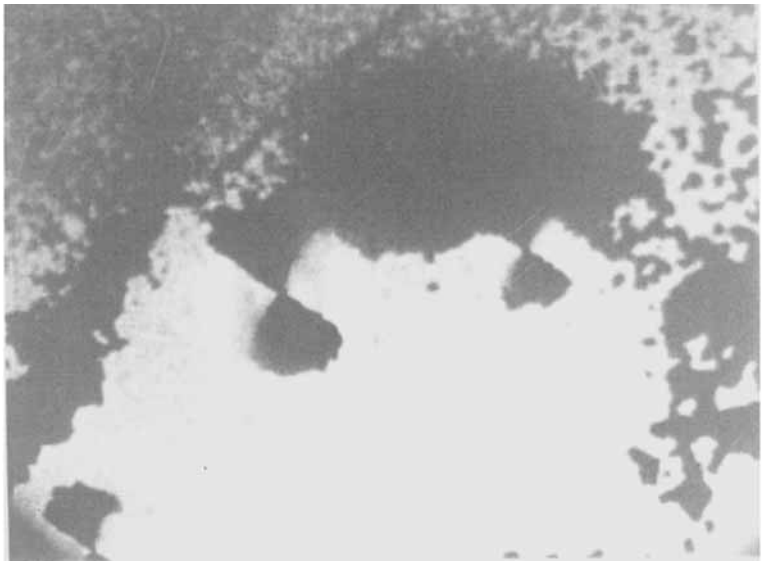

FIGURE 11 E9/muscovite interface. Anchoring patterns due to strains in the vicinity of defects (inclusions). See Color Plate XV.

by an arbitrary number of appropriate chemical species, any useful model of anchoring transition cannot be based on explicit dependence of ω on thermodynamic parameters.

Instead of such a "direct" model, a mean-field model has been proposed in which one proceeds in two steps:

1st—one develops ω into a limited Fourier series (for planar anchorings):

$$\omega = \sum_n (a_n \cos(n\varphi) + b_n \sin(n\varphi)) \tag{15}$$

(or into a series of spherical harmonics in the general case). The coefficients a_n and b_n are treated as independent variables and the search for minima of can be done exactly. As a result, one gets an anchoring diagram in the l-dimensional Fourier space, where l is the number of Fourier coefficients taken into account.

2nd—one introduces the dependence of the coefficients a_n and b_n on suitable thermodynamic variables and projects the anchoring diagram from the Fourier space into the space of physical variables.

In such a procedure, the identity of anchoring transitions is related to singular manifolds in Fourier space.

A typical example of an anchoring diagram in a tri-dimensional Fourier space (a_2, a_4, a_6) is given in Figure 12. As in the search for minima of the series (15) one is interested only in relative depths, the amplitude of can be normalized by an additional condition:

$$a_2^2 + a_4^2 + a_6^2 = 1 \tag{16}$$

so that the diagram shows only the unit sphere. For each point on the sphere, the minimum of the series (15), with respect to φ, was found and the corresponding anchoring angle φ_{min} was represented by a color spot on the sphere. The color code for angles is visualized in the background of the Figure 12. Figure 12b shows schematically division of the anchoring diagram by lines of anchoring transitions. The diagram is divided into three domains I, II and III. The transition between the domains I and II is of first-order because it involves a discontinuous change in the angle of 90 degrees which preserves the symmetry G_a $(= C_s)$. Transitions I $\rightarrow$ III and II $\rightarrow$ III break the mirror symmetry so that, in principle, can be of second-order. In fact, the transition line L_2 changes its character from second- to first order at the tricritical point C_3.

Clearly, by an appropriate projection onto the ternary diagram of Figure 8 one can obtain the lines AA′ and BB′.[20,11] In order to obtain the line CC′ one must suppose that the symmetry of the mica surface is broken from C_s into C_1.[20,11]

Beyond Landau-type phenomenological models, microscopic nature of anchoring transitions should be elucidated. Recent achievements, in visualizing liquid crystal molecules adsorbed on graphite, by means of the scanning tunneling microscope, open new interesting possibilities in this direction.

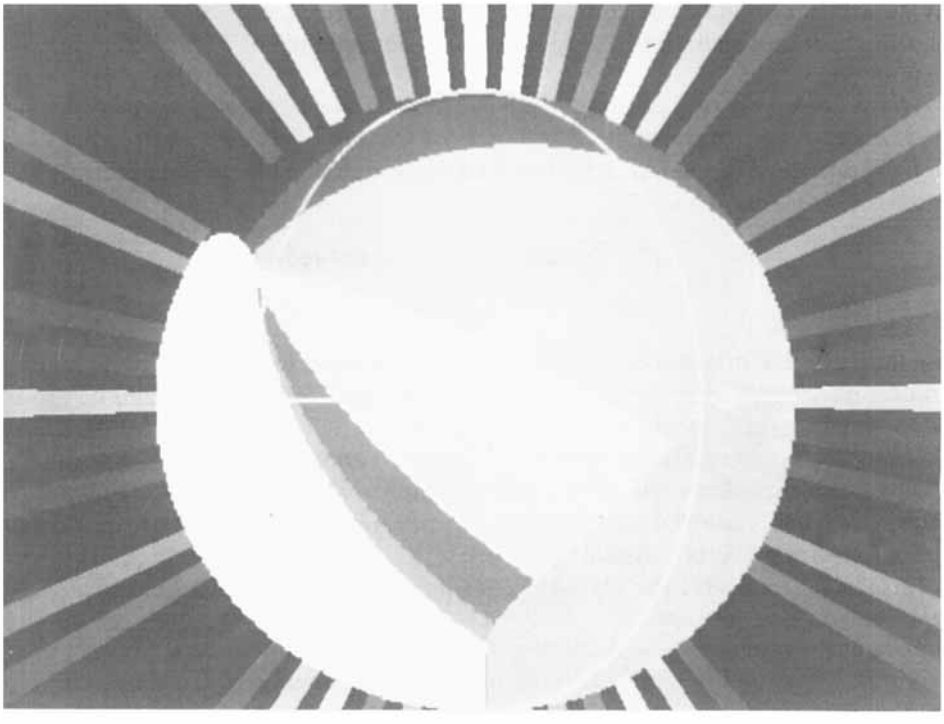

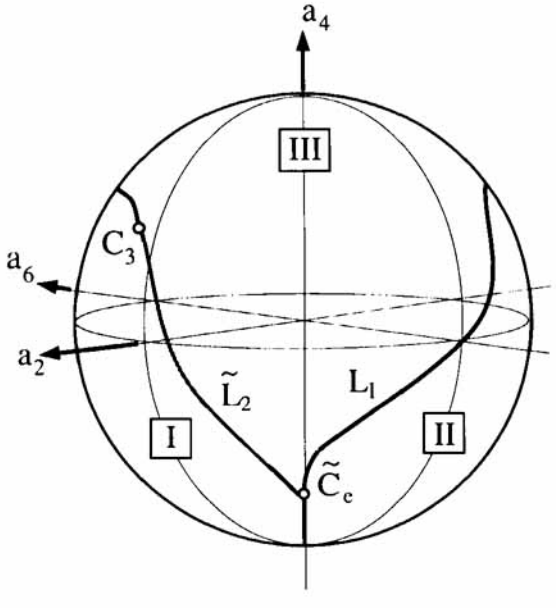

FIGURE 12 Anchoring diagram in Fourier space (a_2, a_4, a_6). See Color Plate XVI.

Acknowledgment

The authors would like to thank The Wissenschaftskolleg zu Berlin and the Technical University Berlin for their very kind hospitality.

References

1. C. Mauguin, *Bull. Soc. Fr. Cryst.*, **34**, 71 (1911).
2. F. Grandjean, *Bull. Soc. Fr. Cryst.*, **39**, 164 (1916).
3. J. Cognard, *Mol. Cryst. Liq. Cryst.*, Suppl. 1, 1 (1982).
4. L. M. Blinov, E. I. Kats and A. A. Sonin, *Sov. Phys. Usp.*, **30**, 604 (1987).
5. H. Yokoyama, *Mol. Cryst. Liq. Cryst.*, **165**, 265 (1988).
6. B. Jérôme, to be published in Rep. Prog. Phys.
7. R. Pandit, M. Schick, M. Wortis, *Phys. Rev.*, **B26**, 5112 (1982).
8. J. W. Gibbs, "On the equilibrium of heterogeneous substances" in *Scientific Papers*, Vol. 1, p. 55, (Longmans, Green and Co. 1906).
9. P. Pieranski, B. Jérome and M. Gabay, *Mol. Cryst. Liq. Cryst.*, **179**, 285 (1990).
10. B. Jérôme and P. Pieranski, *J. de Phys.*, **49**, 1601 (1988).
11. H. Kitzerow, B. Jérôme and P. Pieranski, to be published in *Proc. Conf. Order in Liquids*, Berlin 1990.
12. K. Hiltorp and H. Stegemeyer, *Ber. Bunsenges. Phys. Chem.*, **85**, 582 (1981).
13. G. Ryschenkow and M. Kleman, *J. Chem. Phys.*, **64**, 404 (1976).
14. S. Faetti, *Mol. Cryst. Liq. Cryst.*, **179**, 217 (1990).
15. See for example, T. J. Sluckin and A. Poniewierski, "Orientational wetting phenomena in nematics," in *Fluid Interfacial Phenomena*, edited by C. A. Croxton, John Wiley & Sons.
16. B. Jérôme, P. Pieranski and M. Boix, *Europhys. Lett.*, **5**, 693 (1988).
17. M. Monkade, M. Boix and G. Durand, *Europhys. Lett.*, **5**, 697 (1988).
18. A. Braslau, M. Petrov, A. M. Levelut and G. Durand, unpublished.
19. P. Pieranski and B. Jérôme, *Phys. Rev.*, **A40**, 317 (1989).
20. J. Bechhoefer, J.-L. Duvail, L. Masson, B. Jérome, R. M. Hornreich and P. Pieranski, *Phys. Rev. Lett.*, **64**, 1911 (1990).
21. P. Pieranski and B. Jérome in *Phase Transitions in Soft Condensed Matter*, edited by T. Riste, NATO ASI Series B, Vol. 211, (Plenum, New York, 1989).
22. J. Bechhoefer, B. Jérome and P. Pieranski, *Phys. Rev.*, **A41**, 3187 (1990).
23. L. M. Blinov and A. A. Sonin, *Mol. Cryst. Liq. Cryst.*, **179**, 13 (1990).
24. R. Barberi, M. Boix and G. Durand, *Appl. Phys. Lett.*, **55**, 2506 (1989).
25. B. Jérôme, A. Bosseboeuf and P. Pieranski, *Phys. Rev.*, **A42**, 6032 (1990).